Voxel Based Topometry: Collapse onto a Sphere or an Ellipsoid?

O. P. Posnansky[1], and N. J. Shah[1,2]

[1]Institute of Neuroscience and Biophysics 3 - Medicine, Research Centre Juelich, Juelich, Germany, [2]Faculty of Medicine, Department of Neurology, RWTH Aachen University, JARA, Aachen, Germany

1. Introduction: Measurement of diffusion in MRI is one of the most sensitive ways to explore the heterogeneity of tissue non-invasively. Small differences in diffusivity within tissue placed in a magnetic field give rise to effects which are well measurable in diffusion weighted MRI. Calculation of the ADC over the various diffusion gradient directions in MRI allows us to investigate the anisotropic properties of tissue using the tensor model [1] or spherical harmonics decomposition [2]. With the aim of contributing to the clarification of the anisotropy and heterogeneity within the voxel, we introduce an alternative blowing compact-surface method leading to the setting the new group of scalar parameters - topological non-integer dimensions [3]. The blowing sphere and ellipsoid are chosen as probing surfaces. Our findings suggest that non-Gaussian distribution of the diffusion signal dominates in the brain and carries more detailed information.

2. Methods: 65 images were acquired on a Siemens 3T Trio scanner using a double-refocused, diffusion-weighted spin echo sequence (TR/TE=10000/92ms, voxel size=(1.8mm)^3, b=800s/mm^2) from a healthy male adult. Sixty diffusion-weighted images, corresponding to the sixty directions of diffusion gradients distributed according to the truncated icosahedral scheme, were used. Additionally, five images with b=0 were randomly acquired between the diffusion-weighted images to factor out the T2–weighting of the signal. 3D anatomical images were obtained using the T1-weighted MP-RAGE sequence (TR/TE=2200ms/3.93ms, flip angle = 15°, FOV=(256mm)^2, matrix = 256x256, BW=130Hz/pixel, 176 sagittal slices, voxel size = (1mm)^3). The ADC profiles were recovered using Eq. 1 and afterwards interpolated for voxels within and outside the brain. The profiles demonstrate a very complex structure, correlated with the anatomical architecture. In the Fig.1 the segmented anatomical image of a transverse slice is shown and the ADC profiles are output for voxels located in different types of tissues and outside of the brain. The structure of the profiles can be analysed by the iterative *blowing surface* method [4,5]. As a probing surface, the blowing sphere was chosen for the isotropic case (Fig.2, upper row). For the anisotropic case, an ellipsoid built on eigenvectors with kept ratio between different eigenvalues was chosen (Fig.2, low row). The key point of this method consists in the step-by-step increase of the characteristic scale over all icosahedra directions from the minimal to the maximal value. During expansion of the surface in the certain direction the growth was stopped if the scale exceeded the acquired ADC profile boundary in a given direction. In the Fig. 2, the 3D process is depicted with some intermediate steps in plane (in these figures the equatorial cross sections of the ADC profiles are presented).

3. Results: We calculated the volume V, surface area S and mean radius R during the blowing sphere and ellipsoid iterative scaling process and compared them to the unit measures by adjusting the power D of the scaling parameter R_i of the surfaces (Eq. 2 and 3; i is an iteration number). For the case of ellipsoid $\lambda_1, \lambda_2, \lambda_3$ are the eigenvalues. The scaling iterative procedure of D-power changes (Fig. 3) exhibits three regimes of behaviour: (I) stable regime (plateau), (II) transition and linear collapsing regime, and (III) recovered stable regime (plateau). The linear collapsing regime approaches the attractor points corresponding to the random surface (ADC profile). In the stable regime (I) for the volume, surface and mean radius values D-power was 3, 2 and 1 correspondently. These are the dimensions of the initial, non-corrupted iteratively blown surfaces. Collapsing regime (II) of non-integer topological indices demonstrates *geometrical contrast* between the sphere and the ellipsoid (Fig. 3). Contrast is clearly depicted in the maps of the collapsed parameters (attractor points of D-power) which are presented in Fig. 4 (c,e,g correspond to the ellipsoid and d,f,h correspond to the sphere). For comparison, we also present fractional anisotropy (FA) and normalised mean diffusivity (MD) maps as well in Fig.4a,b respectively.

$$S/S_0 = e^{(-b\cdot ADC)} \quad (1) \qquad M\big|_{M=V,S,R} \sim R_i^D \quad (2) \qquad V \sim R_i^D(\lambda_1\lambda_2\lambda_3) \quad (3a) \qquad S \sim R_i^D(\lambda_1\lambda_2 + \lambda_1\lambda_3 + \lambda_2\lambda_3) \quad (3b) \qquad R \sim R_i^D(\lambda_1 + \lambda_2 + \lambda_3) \quad (3c)$$

4. Discussion: We present a method to characterize the complex structure of the ADC profiles. The key point of the method comprises the iterative scaling of the blowing surfaces: a sphere and an ellipsoid. With the use of the proposed method, a new set of parameters were mapped. These parameters represent the topology of the ADC profiles and correlate with the anatomical structure of the brain. The method provides a novel approach that may enhance the utility and specificity of the diffusion-weighted MRI to better assess the structural changes that occur during the development and progression of various neuropathologies.

References: [1] Basser P.J. et al, *Biophys. J.* 66(1) 1994, 259-267. [2] Tournier J.D. et al, *Neuroimage* 23(3) 2004, 1176-1185. [3] Mandelbrot B., *Fractal Geometry in Nature*, New York (Freeman), 1982. [4] Posnansky O., Shah N.J., *ISMRM* 2008, 1784. [5] Posnansky O., Kupriyanova Y., Shah N.J., *ESMRMB* 2008, 633.

Fig.1

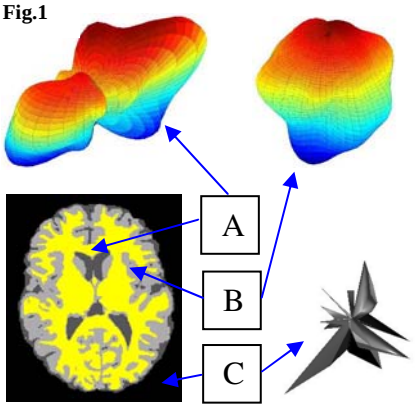

Fig.2

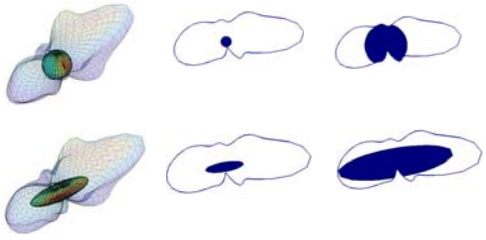

Fig.3

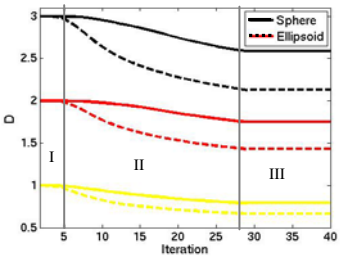

Fig.1. A segmented anatomical image of a transverse slice with typical ADC profiles: A-white matter profile; B-grey matter profile; and C-noise.
Fig.2. Depiction of the blowing surface method: upper row for the sphere; low row for the ellipsoid.

Fig.4

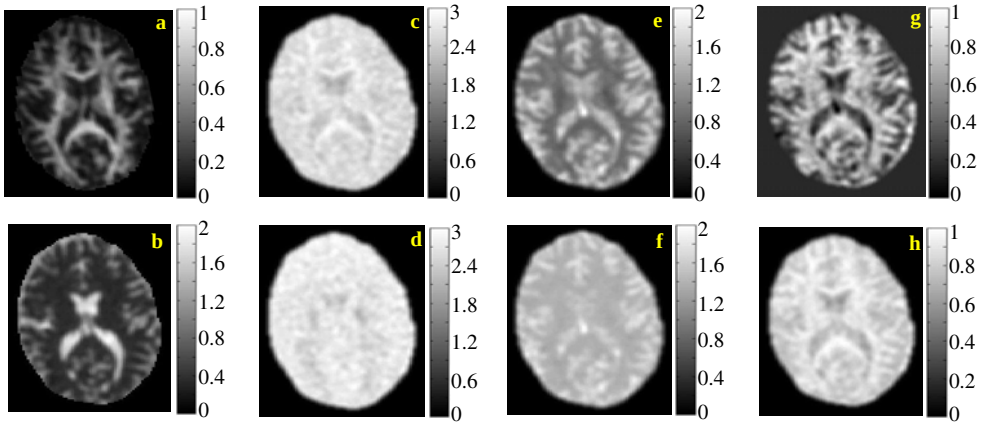

Fig.3. Collapsing of topological indices curves. Solid curve is for the sphere and dashed curve is for the ellipsoid. Differences between the curves for sphere and ellipsoid demonstrate *geometrical contrast.*
Fig.4. (a) FA map; (b) normalised MD map; (c) volume index map for the ellipsoid; (d) volume index map for the sphere; (e) surface area index map for the ellipsoid; (f) surface area index map for the sphere; (g) mean radius index map for the ellipsoid; (h) mean radius index map for the sphere.